

# Journal Pre-proof

Comparative study of direct methylation of benzene with methane on cobalt-exchanged ZSM-5 and ZSM-11 zeolites

Peidong Hu (Methodology) (Investigation) (Formal analysis) (Validation) (Data curation) (Visualization) (Writing - original draft), Koshiro Nakamura (Methodology) (Investigation) (Formal analysis) (Validation) (Data curation), Hitoshi Matsubara (Methodology) (Investigation) (Formal analysis) (Validation) (Data curation), Kenta Iyoki (Resources) (Supervision) (Visualization) (Writing - review and editing), Yutaka Yanaba (Investigation), Kazu Okumura (Investigation) (Formal analysis), Tatsuya Okubo (Resources) (Writing - review and editing), Naonobu Katada (Methodology) (Resources) (Conceptualization) (Supervision) (Project administration) (Funding acquisition) (Visualization) (Writing - review and editing), Toru Wakihara (Methodology) (Resources) (Conceptualization) (Supervision) (Project administration) (Funding acquisition) (Visualization) (Writing - review and editing)



PII: S0926-860X(20)30254-4  
DOI: <https://doi.org/10.1016/j.apcata.2020.117661>  
Reference: APCATA 117661

To appear in: *Applied Catalysis A, General*

Received Date: 13 March 2020  
Revised Date: 20 May 2020  
Accepted Date: 21 May 2020

Please cite this article as: Hu P, Nakamura K, Matsubara H, Iyoki K, Yanaba Y, Okumura K, Okubo T, Katada N, Wakihara T, Comparative study of direct methylation of benzene with methane on cobalt-exchanged ZSM-5 and ZSM-11 zeolites, *Applied Catalysis A, General* (2020), doi: <https://doi.org/10.1016/j.apcata.2020.117661>

This is a PDF file of an article that has undergone enhancements after acceptance, such as the addition of a cover page and metadata, and formatting for readability, but it is not yet the definitive version of record. This version will undergo additional copyediting, typesetting and review before it is published in its final form, but we are providing this version to give early visibility of the article. Please note that, during the production process, errors may be discovered which could affect the content, and all legal disclaimers that apply to the journal pertain.

© 2020 Published by Elsevier.

## Comparative study of direct methylation of benzene with methane on cobalt-exchanged ZSM-5 and ZSM-11 zeolites

Peidong Hu,<sup>a</sup> Koshiro Nakamura,<sup>b</sup> Hitoshi Matsubara,<sup>b</sup> Kenta Iyoki,<sup>a,\*</sup>  
Yutaka Yanaba,<sup>c</sup> Kazu Okumura,<sup>d</sup> Tatsuya Okubo,<sup>a</sup> Naonobu Katada,<sup>b,\*</sup>  
Toru Wakihara<sup>a,\*</sup>

<sup>a</sup> *Department of Chemical System Engineering, The University of Tokyo, 7-3-1 Hongo, Bunkyo-ku, Tokyo 113-8656, Japan*

<sup>b</sup> *Center for Research on Green Sustainable Chemistry, Tottori University, 4-101 Koyama-cho Minami, Tottori 680-8552, Japan*

<sup>c</sup> *Institute of Industrial Science, The University of Tokyo, 4-6-1 Komaba, Meguro-ku, Tokyo 153-8505, Japan*

<sup>d</sup> *Department of Applied Chemistry, Faculty of Engineering, Kogakuin University, 2665-1 Nakano-machi, Hachioji, Tokyo 192-0015, Japan*

\* *Corresponding author:*

Kenta Iyoki, Assistant Professor.

E-mail: k\_iyoki@chemsys.t.u-tokyo.ac.jp

Naonobu Katada, Professor.

Tel/Fax: +81-857-31-5684

E-mail: katada@tottori-u.ac.jp

Toru Wakihara, Professor.

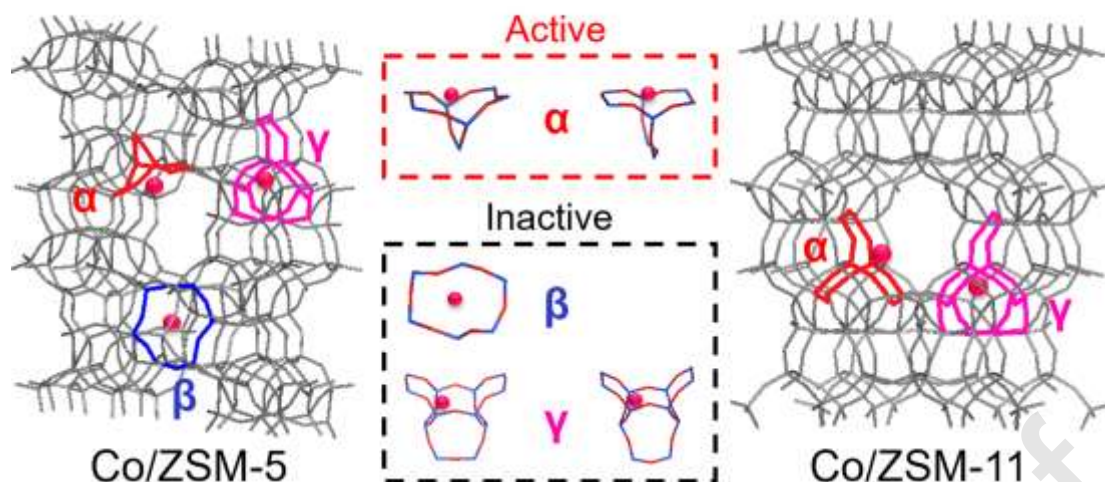
Tel: +81-3-5841-7368

Fax: +81-3-5800-3806

E-mail: wakihara@chemsys.t.u-tokyo.ac.jp

Graphical abstract

## Direct methylation of benzene with methane



### Highlights

- Non-oxidative methylation of benzene with methane was achieved on Co-exchanged ZSM-11.
- More Co<sup>2+</sup> ions were stabilized on ZSM-11 than ZSM-5 with the same Si/Al molar ratio.
- Superior toluene formation rate and turnover frequency were gained on Co-ZSM-11.
- Co<sup>2+</sup> with two main coordination states existed in ZSM-5 and ZSM-11 with different distribution.
- Co<sup>2+</sup> with loose coordination to framework oxygen atoms was critical for the reaction.

### Abstract

Methane exists in massive quantity on the Earth, and considerable efforts have been made to develop effective methods to convert chemically inert methane into value-added products. Recently, cobalt-exchanged ZSM-5 zeolite has been found to be a competent catalyst for non-oxidative methylation of benzene using methane as a methylation agent. Herein, cobalt-exchanged ZSM-11 zeolite, with close topological

structure to that of ZSM-5 zeolite, was discovered to be capable of catalyzing non-oxidative methylation of benzene with methane for the first time. ZSM-5 and ZSM-11 zeolites both with Si/Al molar ratio of ca. 36 and 18 were synthesized. However, higher cobalt loadings were obtained on ZSM-11 zeolites, and cobalt-exchanged ZSM-11 catalysts displayed superior toluene production rates and turnover frequencies. In addition, low silica zeolite catalysts possessed higher methylation selectivity. Diffuse reflectance visible-near infrared spectra revealed that divalent cobalt cations on the ion exchange sites existed mainly in two different coordination states, and the cobalt cation on the  $\alpha$  site, coordinating weakly to the framework oxygen atoms, was supposed to be the active site because of the positive correlation of its concentration and the methane activation performance. Since more  $\alpha$ -type  $\text{Co}^{2+}$  could be created in ZSM-11 zeolites than in ZSM-5 zeolites with the same Si/Al molar ratio, it was concluded that cobalt-exchanged ZSM-11 catalyst was a promising candidate for the non-oxidative methylation of benzene with methane.

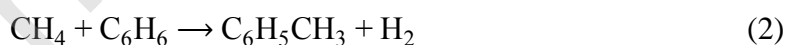
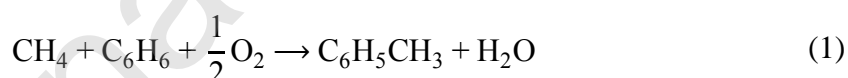
**Keywords:** non-oxidative methane activation; benzene methylation; ZSM-5; ZSM-11; cobalt ion exchange

## 1. Introduction

Fine chemical industry plays a critical role in economic and social development, which is closely related to pharmaceuticals, biomaterials, dyestuffs, textiles, and so on [1]. Alkylaromatic compounds are commonly indispensable reactants in the fine chemical production, among which toluene is one of the most important intermediates. Currently, alcohols, alkenes and haloalkanes are used for the alkylation of benzene to produce alkylaromatic compounds [2]. However, it would be more economically attractive to utilize abundant and low-cost alkanes as alkylation agents instead. Natural gas, whose main component is methane, is an abundant and accessible resource in nature, and is regarded as promising energy source and chemical feedstock besides petroleum. Therefore, the catalytic conversion of methane to higher hydrocarbons is of

great importance not only due to the potential for liquefaction of natural gas for transportation and storage, but also because of the full utilization of its hydrocarbon resource rather than burning as fuel [3].

Nevertheless, the direct chemical activation of methane is much more difficult than other light alkanes, owing to the high dissociation energy of its C–H bond ( $\sim 440$  kJ mol<sup>-1</sup>), low electron and proton affinity, high ionization potential (12.5 eV), and low polarizability [4-6]. The methylation reaction of benzene and methane used to be achieved through the indirect route in an oxidative atmosphere (**Eq. (1)**) [7-9], where methane is first partially oxidized to methoxy species (e.g., methanol) by oxidizing gases like O<sub>2</sub>, and then reacts with benzene to form toluene catalyzed by the acidic sites in the zeolitic catalysts, such as MCM-41, H-beta, H-ZSM-5 and transition metal ion-exchanged zeolites (like Cu, Zn and Co) [10]. The intermediate methoxy species can readily attack benzene to produce methylated products via the electrophilic substitution reaction [7]. Nevertheless, because the methoxy species are much more reactive under the extreme conditions required for the methane activation, and are easier to be adsorbed on the surface of the catalysts due to the molecular polarity, the partial oxidization of methane faces major challenges, such as poor selectivity and side reactions, resulting in the deep oxidation to form thermally stable CO<sub>2</sub> and H<sub>2</sub>O [11, 12].



In recent decades, strenuous efforts have been made to develop direct non-oxidative methods for the conversion of methane into value-added hydrocarbons [5, 13, 14]. The direct methylation of benzene with methane in the non-oxidative atmosphere (**Eq. (2)**) has been discovered to occur over metal-containing ZSM-5 (MFI-type) zeolites, including Pt-ZSM-5, In-ZSM-5 and Ag-ZSM-5 [15-17], in the presence of excessive methane. Very recently, ZSM-5 zeolites with cobalt modified by either ion exchange method or impregnation method were found to display extraordinary catalytic activity for the direct methylation of benzene with methane compared with other

zeolites with different topological structures or metal species [18, 19]. The previous results suggest that ZSM-5 zeolite is particularly useful in the catalytic methylation process with methane.

ZSM-5 zeolite is one of the most extensively studied aluminosilicate zeolites in the pentasil family [20, 21], and is widely applied in the petroleum industry. It possesses a special channel structure with vertical straight channel intersected with horizontal sinusoidal channel [22]. Actually, ZSM-11 (MEL-type) zeolite, another kind of pentasil zeolite, has a very similar structure to that of ZSM-5 zeolite, with two-dimensional intersecting straight channel and almost the same pore-opening size (approximately 0.55 nm) [22]. Some researchers have found that ZSM-11 zeolites also showed activity in the alkylation reactions of various aromatic substrates, such as benzene alkylation with dimethyl ether [23] and toluene alkylation with methanol [24]. To the best of our knowledge, the performance of ZSM-11-based catalysts in the non-oxidative methylation of benzene using methane as the alkylation agent has never been investigated.

In this study, cobalt-exchanged ZSM-5 and ZSM-11 zeolites with two different Si/Al ratios were prepared, and their catalytic performances in the direct methylation of benzene with methane were evaluated. The distribution of divalent cobalt cations on the different ion exchange sites in these zeolites was extrapolated to have great effects on the methane activation. ZSM-11 zeolites could create more active cobalt species than ZSM-5 zeolites with the same Si/Al molar ratio, and consequently cobalt-exchanged ZSM-11 catalysts exhibited higher activity, which could serve as a promising candidate for the target reaction.

## 2. Experimental

### 2.1. Materials

Aluminum chloride hexahydrate ( $\text{AlCl}_3 \cdot 6\text{H}_2\text{O}$ ), sodium hydroxide (NaOH), tetrabutylammonium bromide (TBABr), ammonium nitrate ( $\text{NH}_4\text{NO}_3$ ), cobalt nitrate hexahydrate ( $\text{Co}(\text{NO}_3)_2 \cdot 6\text{H}_2\text{O}$ ), and benzene ( $\text{C}_6\text{H}_6$ ) were purchased from FUJIFILM Wako Pure Chemical Corporation. Colloidal silica (LUDOX<sup>®</sup> AS-40, 40% suspension

in water), and tetrapropylammonium bromide (TPABr) were obtained commercially from Sigma-Aldrich Corporation. Methane (CH<sub>4</sub>) was supplied by Iwatani Corporation. All the chemicals were used without further purification.

## 2.2. Preparation of the catalysts

ZSM-5 (Z5) and ZSM-11 (Z11) zeolites were synthesized through the conventional hydrothermal method. Typically, AlCl<sub>3</sub>·6H<sub>2</sub>O was dissolved in water, followed by the addition of NaOH and organic structure-directing agent (OSDA) to form a clear solution. TPABr and TBABr were used as OSDAs for the syntheses of ZSM-5 and ZSM-11 zeolites, respectively. Then, colloidal silica was added dropwise into the aforementioned solution and a white reactant was obtained, which was stirred vigorously and transferred into a Teflon<sup>®</sup>-lined stainless steel autoclave (No. 4749, Parr Instrument Company). The composition of the reactant was  $x\text{SiO}_2: 1.23\text{Al}_2\text{O}_3: 12\text{Na}_2\text{O}: 2(\text{TBA}_2\text{O or TPA}_2\text{O}): 3600\text{H}_2\text{O}$ , where  $x = 95$  and  $50$  for the products with high Si/Al molar ratio (Z5-HS and Z11-HS) and low Si/Al molar ratio (Z5-LS and Z11-LS), respectively. The hydrothermal treatment was carried out at 160 °C with a rotation rate of 40 rpm. After the reaction finished, the reactor was cooled by water, and the white products were collected by vacuum filtration, washed with deionized water, and dried at 80 °C. The as-synthesized products were further calcined at 550 °C for 5 h to remove the OSDAs.

The calcined products were first ion exchanged with NH<sub>4</sub>NO<sub>3</sub> solution (1 M) once to obtain NH<sub>4</sub><sup>+</sup>-type zeolites, and then ion exchanged with Co(NO<sub>3</sub>)<sub>2</sub> solution (0.05 M) twice to obtain cobalt-exchanged zeolites. The ion exchange experiments were conducted at 70 °C for 4 h, and the solid to liquid ratio was 1:100 (g/mL).

## 2.3. Characterization

The X-ray diffraction (XRD) patterns were obtained on a Rigaku Ultima IV diffractometer using a Cu K $\alpha$  radiation source (40 kV, 40 mA). The solid-state <sup>27</sup>Al magic angle spinning nuclear magnetic resonance (MAS NMR) spectra were recorded on a JNM-ECA 500 (JEOL) spectrometer at a spinning rate of 17 kHz with a  $\pi/12$  pulse width of 0.5  $\mu$ s and a relaxation delay of 0.1 s by scanning 10000 times. The *in situ* Fourier transform infrared (FT-IR) spectra of the dehydrated proton-type samples were

gained on a JASCO FT/IR-4700 spectrometer. The ammonium-type samples were compressed into a self-supporting disk of 10 mm diameter, and pretreated in O<sub>2</sub> flow inside an *in situ* IR cell with CaF<sub>2</sub> window at 550 °C for 1 h to remove water and convert to proton-type before cooled down in Ar flow, and the spectra were collected at 100 °C. The textural properties were evaluated by the nitrogen adsorption–desorption analyses on a Quantachrome Autosorb-iQ2-MP at liquid nitrogen temperature (77 K). Before the measurements, the samples were pretreated at 325 °C for 4 h under vacuum. The morphologies of the samples were observed by a field-emission scanning electron microscope (FE-SEM, JSM-7000F, JEOL). The chemical compositions of the samples were analyzed by inductively coupled plasma atomic emission spectroscopy (ICP-AES, Thermo iCAP 6300), after the samples were dissolved in hydrofluoric acid solution. The X-ray absorption spectroscopy (XAS) measurements were performed at beamline BL9C in KEK-PF, Japan, under the approval of the Photon Factory Program Advisory Committee (Proposal No. 2018G628). The samples were compressed into a 10-mm-diameter wafer. The Co K-edge absorption spectra were collected in the quick scan mode using a Si(111) monochromator at room temperature in the atmosphere. The diffuse reflectance ultraviolet-visible-near infrared (DR UV-Vis-NIR) spectra of the cobalt-exchanged samples were recorded on a JASCO V-770 spectrophotometer in the wavelength range of 190–2700 nm with BaSO<sub>4</sub> as the reference. Before the measurements, the samples were compressed into a tablet and dehydrated at 500 °C for 1 h under low pressure (1 Pa).

#### 2.4. Evaluation of catalytic performance

The temperature-programmed reaction experiments in the temperature range of 100–570 °C were carried out in a fixed-bed flow reactor with 0.3 g catalyst according to the procedures reported in the previous paper [25]. After the pretreatment in O<sub>2</sub> flow (1.48 mmol min<sup>-1</sup>) at 550 °C for 1 h, the system was cooled to 100 °C. Then, the gas flow was changed to a mixture of He (84.6 μmol min<sup>-1</sup>), CH<sub>4</sub> (1.23 mmol min<sup>-1</sup>) and C<sub>6</sub>H<sub>6</sub> (53.1 μmol min<sup>-1</sup>), and the experiment was initiated when the temperature was raised at a ramp rate of 10 °C min<sup>-1</sup>. The gas species flowing out of the reactor were detected by mass spectrometry (MS, Pfeiffer Vacuum QMS 200). The pretreatment in

O<sub>2</sub> atmosphere will not influence the Co<sup>2+</sup> cations stabilized on the ion exchange sites.

The long-term catalytic performances were evaluated at 540 °C in the same system as that in the temperature-programmed reaction experiments, after the pretreatment conducted in nitrogen atmosphere at 550 °C for 1 h. Thermogravimetric analyses of the spent catalysts were performed on a Rigaku Thermo plus TG 8120 thermogravimeter under a flow of 10% O<sub>2</sub>/90% He mixed gas at a heating rate of 10 °C min<sup>-1</sup>.

### 3. Results and discussion

#### 3.1. Physicochemical properties of the catalysts

In this study, ZSM-5 and ZSM-11 zeolites were synthesized through a facile hydrothermal method using the same reactant composition but different OSDAs, i.e., TPA<sup>+</sup> and TBA<sup>+</sup>, respectively. The difference of the properties between the synthesized zeolites caused by the synthetic method could be eliminated. The manipulation of Si/Al molar ratios in the final samples was realized by altering the amount of silica source added in the reactants with other parameters unchanged (**Table 1**). XRD patterns of the different samples after calcination are depicted in **Fig. 1(a)**. ZSM-5 zeolites feature triplet diffraction peaks in the  $2\theta$  range of 22–25°, representing the typical MFI topological structure, while ZSM-11 zeolites with MEL topological structure exhibit only two diffraction peaks in the same  $2\theta$  range. Although syntheses of ZSM-11 zeolites are usually accompanied with the formation of ZSM-5 impurity, the absence of the diffraction peak at approximately 24.4° and the doublet peaks at 45.5°, which are characteristic for ZSM-5 impurity [26], indicates the successful synthesis of ZSM-11 zeolites with high purity.

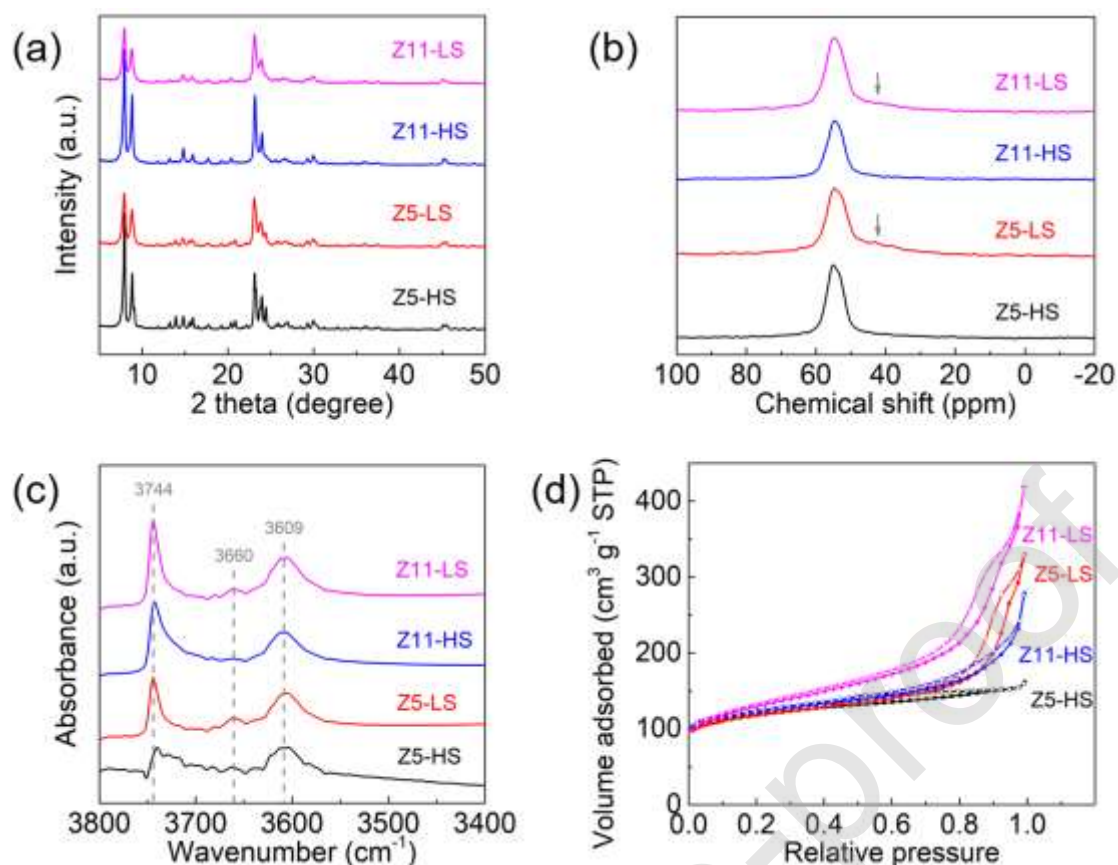


**Fig. 1.** (a) XRD patterns, (b) solid-state  $^{27}\text{Al}$  MAS NMR spectra (the broad signal related to perturbed Al tetrahedra is indicated by arrow), (c) *in situ* FT-IR spectra, and (d) nitrogen adsorption (closed symbols)–desorption (open symbols) isotherms of the samples.

**Table 1.** Chemical compositions, textural properties and Co distributions of the samples.

	Si/Al <sup>a</sup>	Co/Al <sup>a</sup>	$V_{\text{micro}}^{\text{b}}$ ( $\text{cm}^3 \text{g}^{-1}$ )	Co content (wt%)	Co distribution <sup>c</sup> (%)		
					$\alpha$ site	$\beta$ site	$\gamma$ site
CoZ5-HS	36	0.23	0.16	0.62	39	58	3
CoZ5-LS	18	0.29	0.16	1.49	21	76	3
CoZ11-HS	36	0.37	0.17	0.96	44	54	2
CoZ11-LS	17	0.36	0.16	1.98	31	65	4

<sup>a</sup> Determined by ICP-AES.

<sup>b</sup> Volume of the pore with diameter less than 0.57 nm calculated from the calcined Na-form products.

<sup>c</sup> Calculated based on the results of DR Vis-NIR spectra.

According to the solid-state <sup>27</sup>Al MAS NMR spectra (**Fig. 1(b)**), all the samples show a main resonance peak with a chemical shift of approximately 55 ppm, which is attributed to the framework tetrahedral aluminum species, and the octahedrally coordinated aluminum species characterized by a resonance signal at about 0 ppm are not detected. For the zeolites with higher Al contents, Z5-LS and Z11-LS, an additional broad signal with low intensity in the range of 30–50 ppm is found, indicating the presence of a minor number of perturbed Al tetrahedra in the less ordered environment [27, 28]. Meanwhile, in the *in situ* FT-IR spectra of the dehydrated proton-type zeolites in the region of OH stretching vibrations (**Fig. 1(c)**), in addition to the two major peaks corresponding to the external silanol sites (3744 cm<sup>-1</sup>) and the bridging Si(OH)Al groups (3609 cm<sup>-1</sup>), respectively, Z5-LS and Z11-LS samples also exhibit a weak signal at around 3660 cm<sup>-1</sup>, which is probably related to the terminal (SiO)<sub>3</sub>AlOH groups at the framework defects [28].

FE-SEM images illustrate the morphological differences among the synthesized zeolites (**Fig. 2**). Although the synthetic conditions were the same, the particle size of Z5-HS (2–3 μm), which possesses irregular surface and intergrowth morphology (**Fig. 2(a)**), is larger than that of Z11-HS (0.3–0.5 μm, **Fig. 2(b)**). With the increase of Al content, the particle size of Z5-LS (**Fig. 2(c)**) decreases obviously, corroborating the previous report [29]. Nevertheless, in contrast to ZSM-5, the Si/Al molar ratio has a minor influence on the particle size of ZSM-11 (**Fig. 2(b)** and **(d)**). Nitrogen adsorption–desorption experiments were employed to evaluate the textural properties of the zeolites (**Fig. 1(d)**). Z5-HS and Z11-HS display isotherms of type I, which reflects conventional microporous structures of zeolites. Nevertheless, the isotherms of Z5-LS and Z11-LS with higher Al contents change significantly, and contain type I and IV features with an obvious hysteresis loop and a greater nitrogen uptake at high relative pressures ( $P/P_0 > 0.8$ ), suggesting the hierarchical structure consisting of both micropores and mesopores [30]. Because of the reduced crystal sizes observed in the FE-SEM images, the mesoporosity can be attributed to the interparticle voids formed by

the agglomeration of small crystals [31]. The micropore volumes of these four zeolites are close (**Table 1**), owing to their similarities in the topological structures.

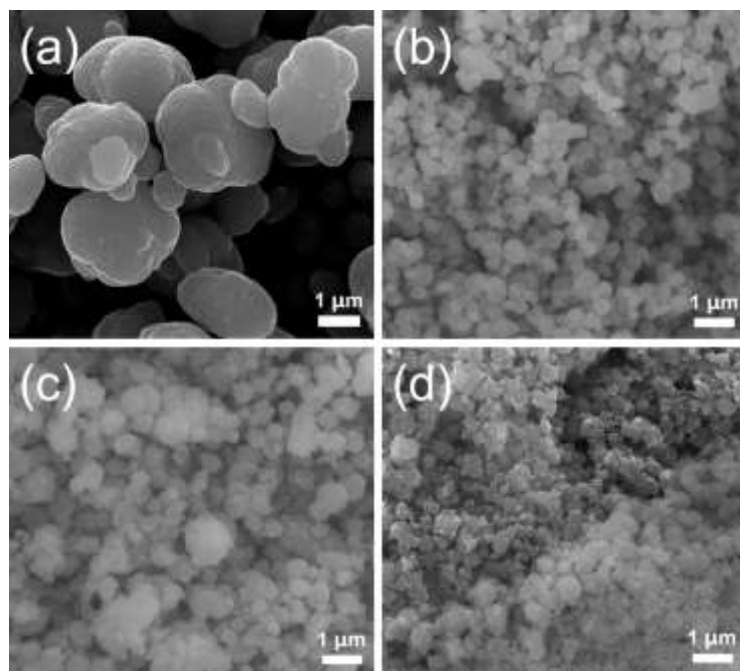


**Fig. 2.** FE-SEM images of (a) Z5-HS, (b) Z11-HS, (c) Z5-LS, and (d) Z11-LS.

The calcined zeolites were subjected to ion exchange in  $\text{NH}_4\text{NO}_3$  solution, followed by additional ion exchange in  $\text{Co}(\text{NO}_3)_2$  solution twice to obtain fully exchanged cobalt-containing samples, and the chemical compositions are summarized in **Table 1**. According to the *in situ* FT-IR spectra (**Fig. S1**), the introduction of Co species has little influence on the OH groups deriving from the external silanol sites ( $3744\text{ cm}^{-1}$ ) and framework Al defects ( $3660\text{ cm}^{-1}$ ), while the intensities of the peaks associated to the bridging Si(OH)Al groups ( $3609\text{ cm}^{-1}$ ) decrease, implying that the  $\text{Co}^{2+}$  cations were balanced by the negative sites created by the framework Al tetrahedra. It is well known that close Al pairs are necessary to stabilize divalent  $\text{Co}^{2+}$  cations, and in the Si-rich zeolites, the ion exchange is generally incomplete, i.e.,  $\text{Co}/\text{Al} < 0.5$ , with part of Brønsted acid sites remaining [32]. The Co/Al molar ratio in ZSM-5 samples slightly increases with the decrease in Si/Al molar ratio, while both high and low silica ZSM-11 samples have a Co/Al molar ratio at approximately 0.36. Meanwhile, the exchange degrees for the ZSM-11 samples are higher than those for the ZSM-5 samples,

which suggests that more Al pairs exist in the ZSM-11 zeolites when the Si/Al molar ratio is the same [33].

The Co K-edge X-ray absorption near edge structure (XANES) spectra of the different cobalt-exchanged zeolites are depicted in **Fig. 3(a)**, along with the reference samples of cobalt with various oxidation states. The absorption edges of all four samples are the same, and their XANES features are close to that of bulk CoO, suggesting that the cobalt loaded in the zeolites via the ion exchange method maintained the oxidation state of +II [19]. Meanwhile, the radial distribution function of Co K-edge extended X-ray absorption fine structure (EXAFS) spectra of the Co-containing zeolites (**Fig. 3(b)**) show only a first-shell peak at 0.16 nm corresponding to the Co–O bond, indicating that the aggregation of Co species did not occur, and the divalent Co cations were monoatomically dispersed in the zeolites [19]. It should be noted that the coordination number of the Co species in these samples can not be directly compared due to the limited quality of the data. In addition, the measurements were carried out at room temperature in the atmosphere, and thus the results do not reflect the working states of the Co species during the catalytic reaction.

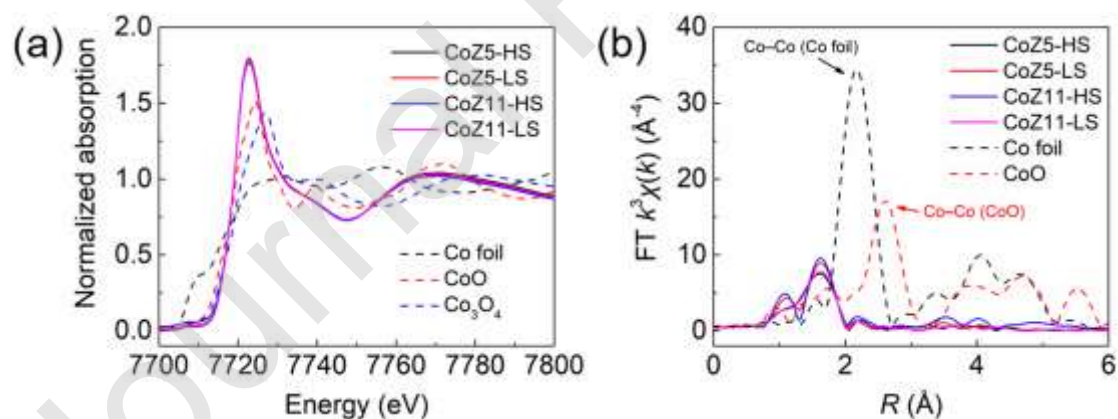


**Fig. 3.** (a) Co K-edge XANES spectra and (b) Fourier transforms of  $k^3$ -weighted ( $k$  range from 3 to 12) EXAFS spectra of cobalt-exchanged zeolites and reference samples.

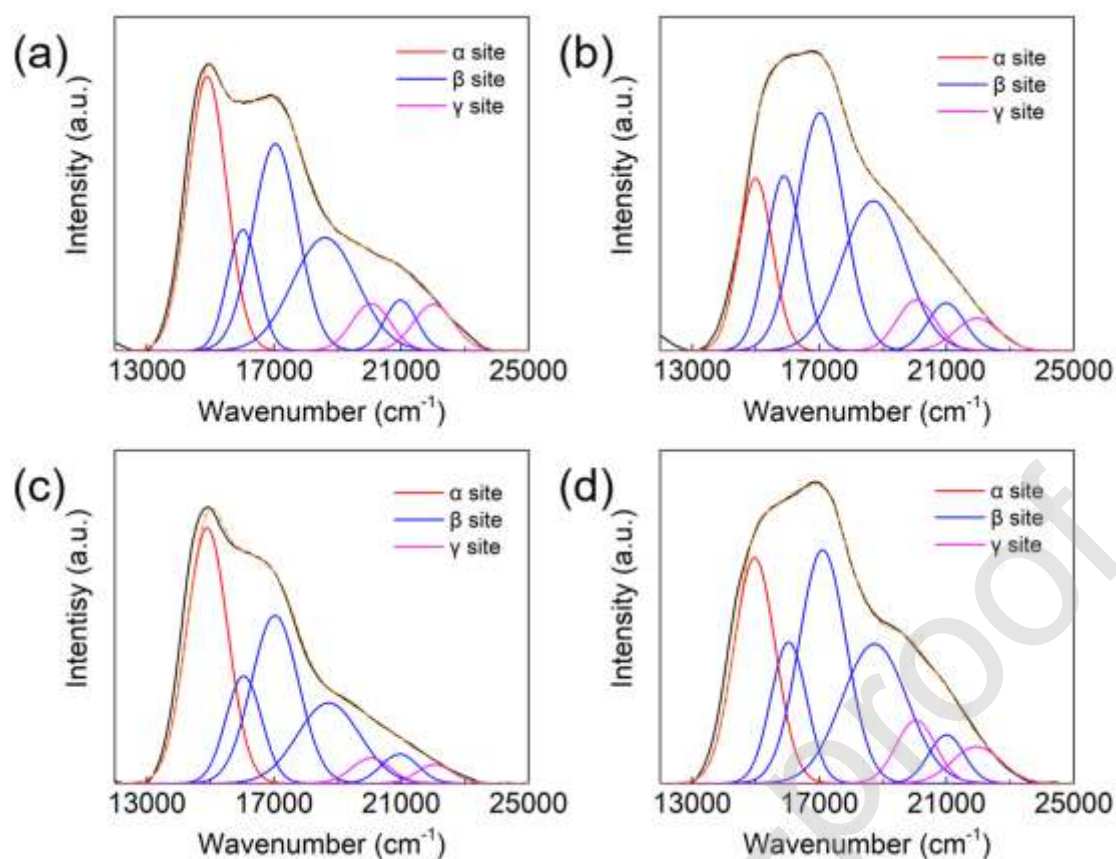


**Fig. 4.** DR Vis-NIR spectra of dehydrated (a) CoZ5-HS, (b) CoZ5-LS, (c) CoZ11-HS, and (d) CoZ11-LS.

DR UV-Vis-NIR spectroscopy of the dehydrated cobalt-exchanged zeolites is commonly employed to evaluate the composition and distribution of the cobalt species in the pentasil-containing high silica zeolites, such as ZSM-5, mordenite, beta, and ferrierite [34], and the results could be close to the states of Co species in the catalysis because of the similar *in situ* high-temperature pretreatment before the measurements. The DR UV-Vis-NIR spectra ( $6000\text{--}38000\text{ cm}^{-1}$ ) of the cobalt-exchanged ZSM-5 and ZSM-11 samples dehydrated at  $500\text{ }^{\circ}\text{C}$  are shown in **Fig. S2**. The absence of the vibrational combination band ( $2\nu$ ) of the water molecule at  $7100\text{ cm}^{-1}$  confirms the complete dehydration of the samples, while the sharp peak at  $7300\text{ cm}^{-1}$  is attributed to the first stretching overtone ( $2\nu$ ) of the skeletal hydroxyl group [35, 36]. Meanwhile, the absorption at approximately  $31500\text{ cm}^{-1}$ , which is related to the charge transfer character of the Co ions with oxygen ligands bounded [36, 37], is insignificant, indicating that the cobalt oxide-like species were negligible in the samples prepared by

the ion exchange method. The absorption band in the visible region reflects the  $d-d$  transitions of the  $\text{Co}^{2+}$  ions in the cationic sites [37]. It has been widely accepted that for the dehydrated cobalt-exchanged ZSM-5 zeolites, this band can be deconvoluted into three spectral components, corresponding to the  $\alpha$  site in the straight channel (single band at  $15100\text{ cm}^{-1}$ ),  $\beta$  site at the intersection of straight and sinusoidal channels (four bands at  $16000$ ,  $17150$ ,  $18600$ , and  $21200\text{ cm}^{-1}$ ), and  $\gamma$  site in the sinusoidal channel (two bands at  $20100$  and  $22000\text{ cm}^{-1}$ ) [32, 34]. However, such assignments in the cobalt-exchanged ZSM-11 zeolites have rarely been reported. Because of the close topological structures of the ZSM-5 and ZSM-11 zeolites, some researchers attempted to process the spectra of the cobalt-exchanged ZSM-11 zeolites similarly to that of ZSM-5 zeolites, but with ambiguous and changeable peak positions [38, 39]. In this study, we deconvoluted the peaks of the cobalt-exchanged ZSM-5 and ZSM-11 samples in the same way according to the previously reported method [34], on the assumption that the corresponding peaks in both zeolites locate at the same position, and the results are depicted in **Fig. 4**. All the samples give a good fit of the experimental spectra, which suggests that the curve fitting method is viable. The fraction of  $\text{Co}^{2+}$  ions on the  $\gamma$  sites is inappreciable for all the samples (**Table 1**). Compared with the high silica samples (CoZ5-HS and CoZ11-HS), the samples with high Al contents (CoZ5-LS and CoZ11-LS) have a higher ratio of  $\text{Co}^{2+}$  ions on the  $\beta$  sites, concurrent with the decreased population of  $\text{Co}^{2+}$  ions on the  $\alpha$  sites, which is in accordance with the previous report [40]. In addition, with the same Si/Al molar ratio, the proportion of  $\text{Co}^{2+}$  ions on the  $\alpha$  sites in the ZSM-11 zeolites is higher than that in the ZSM-5 zeolites. When the cobalt loading is considered, the sequence of the concentration of the  $\text{Co}^{2+}$  on the  $\alpha$  sites is as follows: CoZ11-LS > CoZ11-HS > CoZ5-LS > CoZ5-HS (**Fig. S3**).

### 3.2. Catalytic performance of the catalysts

Since the non-oxidative methylation of benzene with methane (**Eq. (2)**) is thermodynamically infeasible under normal conditions, the reactions were carried out in a methane-rich condition in this study ( $F_{\text{CH}_4}/F_{\text{C}_6\text{H}_6} = 23$  in molar ratio) [10], and the temperature-programmed reaction experiments were conducted to monitor the

formation of toluene, the main product [18, 25], against the reaction temperature in the presence of various catalysts under this condition (**Fig. 5**). When the reaction temperature is below 400 °C, the formation of toluene can hardly be detected, but with a significant production of hydrogen (**Fig. S4**), which corroborates that the dehydrogenation of methane (**Eq. (3)**) prevailed in the low temperature region as a side reaction [18]. The formation of toluene is observed with the increase of reaction temperature above 400 °C, and accelerated in the high temperature region (> 500 °C). CoZ11-LS exhibits the highest toluene formation rate among the four catalysts, followed by CoZ5-LS and CoZ11-HS with close toluene production performances, and CoZ5-HS displays the lowest activity. Therefore, the production of toluene through the methylation of benzene with methane was practical under the experimental conditions at high reaction temperature region (> 400 °C) using the cobalt-exchanged ZSM-5 and ZSM-11 zeolites as the catalysts.

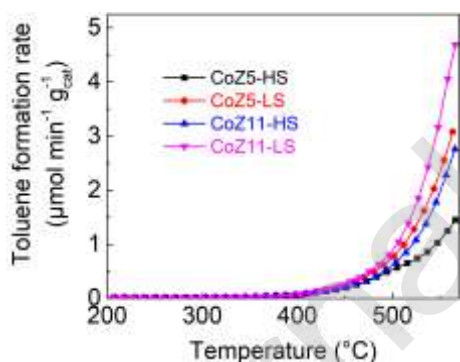


**Fig. 5.** Toluene formation rate on different catalysts as a function of reaction temperature in the methylation of benzene with methane ( $F_{\text{He}}$ ,  $F_{\text{CH}_4}$  and  $F_{\text{C}_6\text{H}_6} = 84.6$ , 1230 and  $53.1 \mu\text{mol min}^{-1}$ , respectively, and  $\text{WHSV}_{\text{C}_6\text{H}_6} = 0.83 \text{ h}^{-1}$ ).

The long-term catalytic performances of the four catalysts for the direct methylation of benzene with methane were further evaluated at 540 °C (**Fig. 6(a)**). The results are similar to that of the temperature-programmed reaction experiments, where CoZ11-LS shows an unparalleled toluene formation rate compared with other three

catalysts. It should be noted that in these four catalysts, the amounts of cobalt, the active species for the catalytic reaction [18, 19], were different even for the ZSM-5 and ZSM-11 zeolites with the same Si/Al molar ratio (**Table 1**). Therefore, the apparent turnover frequencies (TOFs) were calculated according to **Eq. (4)** to compare the toluene formation rates normalized by the cobalt content (**Fig. 6(b)**). It is found that for a certain type of zeolite (ZSM-5 or ZSM-11), the toluene formation rate seems to be proportional to the cobalt content, which is consistent with the previous report [18], and the apparent TOFs for both high and low silica samples are close. Meanwhile, the catalysts using ZSM-11 zeolites as the supports display higher apparent TOFs than those using ZSM-5 zeolites as the supports, corroborating that the cobalt-exchanged ZSM-11 zeolites possessed superior reactivity in the catalytic reaction to produce toluene.

$$\text{Apparent TOF (h}^{-1}\text{)} = \frac{\text{Toluene formation rate } (\mu\text{mol min}^{-1} \text{g}_{\text{cat}}^{-1})}{\text{Cobalt content } (\mu\text{mol g}_{\text{cat}}^{-1})} \times 60 \quad (4)$$

The methane conversions with time on stream for these four zeolite catalysts are illustrated in **Fig. S5(a)**. CoZ11-LS displays the highest methane conversion ability, while CoZ5-HS consumes the least amount of methane, which are consistent with their toluene production performances. However, CoZ11-HS has a higher methane consumption than CoZ5-LS, despite their close toluene formation rates, which hints that the methane utilization rates for the methylation of benzene on the different catalysts were different. As was stated in previous papers [18, 25], besides the target reaction, methane would also dehydrogenate on the Co species to form coke as a side reaction (**Eq. (3)**). According to the methylation selectivity calculated by **Eq. (5)**, low silica zeolite catalysts show a higher methylation selectivity than their corresponding high silica counterparts (**Fig. S5(b)**). The coke amount on the catalysts reflects the combined effects of methane conversion and methylation selectivity. In the thermogravimetric analyses (**Fig. S6**), all the spent catalysts show a weight loss in the temperature range of 300–700 °C. The low silica zeolite catalysts (CoZ5-LS and CoZ11-LS) not only exhibit higher toluene formation rates, the carbon depositions on them are also less than those on the corresponding high silica zeolite catalysts (CoZ5-HS and CoZ11-HS), manifesting their higher methylation selectivities. It is noteworthy

that CoZ5-LS has the least carbon deposition owing to its relatively low methane conversion and high methylation selectivity. In future, the detailed coking pathway and mechanism deserve further investigation.

$$\text{Methylation selectivity (\%)} = \frac{\text{Toluene formation rate } (\mu\text{mol min}^{-1})}{\text{Methane consumption rate } (\mu\text{mol min}^{-1})} \times 100\% \quad (5)$$

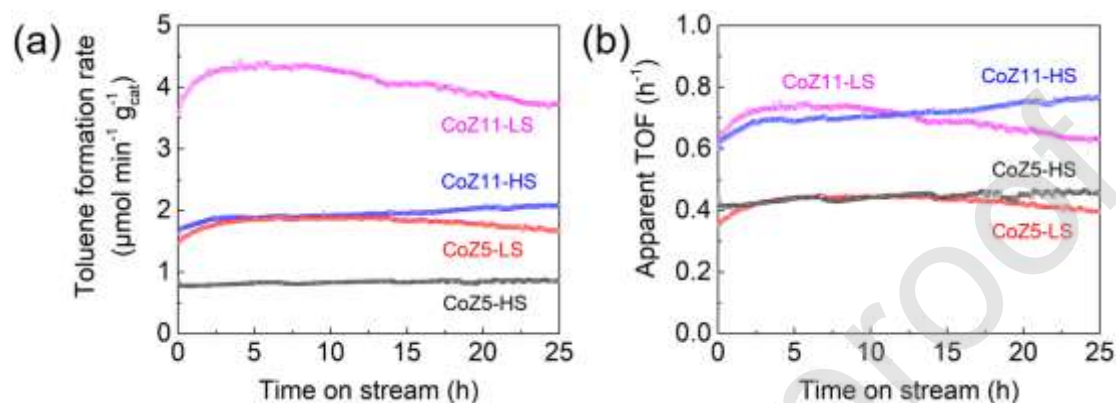


**Fig. 6.** (a) Toluene formation rate and (b) apparent turnover frequency with time on stream for different catalysts in the methylation of benzene with methane at 540 °C ( $F_{\text{He}}$ ,  $F_{\text{CH}_4}$  and  $F_{\text{C}_6\text{H}_6}$  = 84.6, 1230 and 53.1  $\mu\text{mol min}^{-1}$ , respectively, and  $\text{WHSV}_{\text{C}_6\text{H}_6}$  = 0.83  $\text{h}^{-1}$ ).

In this study, the particle sizes of the synthesized ZSM-5 and ZSM-11 zeolites were different (**Fig. 2**), though the precursor reactant composition and the Si/Al molar ratio of the final products were the same. In some cases, particle size has a remarkable influence in the catalytic reactions, and the catalysts with large particle size have stronger diffusion limitations and shorter lifetimes [41, 42]. However, according to the results of the temperature-programmed reactions of the direct methylation of benzene with methane, the toluene formation rates increased rapidly and monotonously in the temperature range of 500–570 °C. Furthermore, the toluene formation rates were insusceptible to the partial pressure of benzene in the presence of excessive methane (data not shown). These results suggest that under the studied conditions, the particle size of the catalysts exerted a minor influence on the apparent activity, and the chemical

reactions on the active sites were probably the rate-limiting step.

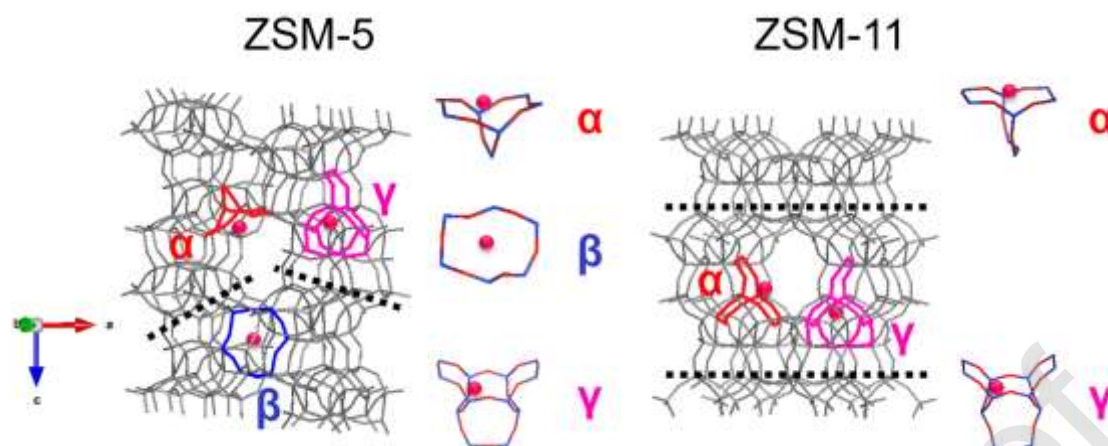


**Fig. 7.** Schematic representation of local framework structures of possible ion exchange sites in ZSM-5 and ZSM-11 zeolites. The straight channel for both zeolites is along  $b$  direction, and the dash line indicates the sinusoidal channel and the other straight channel in ZSM-5 and ZSM-11 zeolites, respectively. The pink ball indicates the cobalt cation. The  $\alpha$ ,  $\beta$  and  $\gamma$  sites in the ZSM-5 zeolites have been widely accepted [34]. In the ZSM-11 zeolites, a same structure as the  $\gamma$  site in the ZSM-5 zeolites can be found. The  $\beta$  site in the ZSM-5 zeolites or its similar structure do not exist in the ZSM-11 zeolites. A similar structure to the  $\alpha$  site in the ZSM-5 zeolites can be found in the ZSM-11 zeolites, but differs in the bridging part, where the  $\alpha$  site in the ZSM-5 zeolites has one T atom and the  $\alpha$  site in the ZSM-11 zeolites has two T atoms. The local arrangement of the  $\alpha$  sites in both zeolites where  $\text{Co}^{2+}$  can access is the same.

It has been already reported that the Lewis acidic divalent cobalt cations on the ion exchange sites in zeolites were believed to be effective for the target reaction [18, 19]. As revealed by the DR Vis-NIR spectra (**Fig. 4** and **Table 1**),  $\text{Co}^{2+}$  cations were mainly located on two kinds of ion exchange sites, namely  $\alpha$  site and  $\beta$  site [34]. In the ZSM-5 zeolites (**Fig. 7**),  $\text{Co}^{2+}$  cations on the  $\alpha$  sites are coordinated to four framework oxygen of the enlarged six-membered ring, while  $\text{Co}^{2+}$  cations on the  $\beta$  sites are closely coordinated to the plane of the deformed six-membered ring [34]. On the other hand, in the ZSM-11 zeolites (**Fig. 7**), the same structure as the  $\beta$  site in the ZSM-5 zeolites

is absent, and a similar structure to the  $\alpha$  site can be found. The presence of the  $\beta$ -type  $\text{Co}^{2+}$  in the DR Vis-NIR spectra of the cobalt-exchanged ZSM-11 zeolites indicates that probably the  $\text{Co}^{2+}$  in a similar coordination state to the  $\beta$ -type  $\text{Co}^{2+}$  in the ZSM-5 zeolites still existed, but with a smaller proportion compared with that in the ZSM-5 zeolites (**Table 1**). Meanwhile, the formation of the  $\alpha$ -type  $\text{Co}^{2+}$  was favorable in the ZSM-11 zeolites. Compared to the  $\beta$ -type  $\text{Co}^{2+}$ , the  $\alpha$ -type  $\text{Co}^{2+}$  has a weaker bonding to the adjacent electronegative framework oxygen atoms, and thus exhibits a stronger Lewis acidity [39, 43]. It has been reported that the electron-donating  $\text{N}_2\text{O}$  molecules preferred to coordinate to the  $\alpha$ -type  $\text{Co}^{2+}$  and were decomposed subsequently [39]. In the present study, the concentration of cobalt on the  $\alpha$  site had a gratifying positive correlation with the methane conversion (**Fig. 8** and **S7**), which should be a critical step in the direct methylation of benzene with methane. Actually, the activation and dissociation of methane are quite difficult considering the poor nucleophilicity for the coordination to metal active sites and the high thermodynamic barrier for the C–H bond cleavage [44, 45], and the  $\alpha$ -type  $\text{Co}^{2+}$  with stronger Lewis acidity helps facilitate the activation of methane. Furthermore, the methane activation performance seems to be enhanced when the concentration of  $\alpha$ -type  $\text{Co}^{2+}$  is high enough (**Fig. S7**). In contrast, CoZ5-LS with high amount of the  $\beta$ -type  $\text{Co}^{2+}$  (the  $\gamma$ -type  $\text{Co}^{2+}$  was not considered due to its extremely low content) did not possess high activity, which demonstrates that probably the  $\beta$ -type  $\text{Co}^{2+}$  is inessential in the studied reaction. These results are also in line with the previous report that active cobalt species for the methylation of benzene with methane were selectively formed in Co/MFI catalysts [19]. Because more  $\alpha$ -type  $\text{Co}^{2+}$  was created in ZSM-11 zeolites than in ZSM-5 zeolites with the same Si/Al molar ratios (**Table 1** and **Fig. S3**), cobalt-exchanged ZSM-11 zeolites were promising catalysts for the direct methylation of benzene with methane.

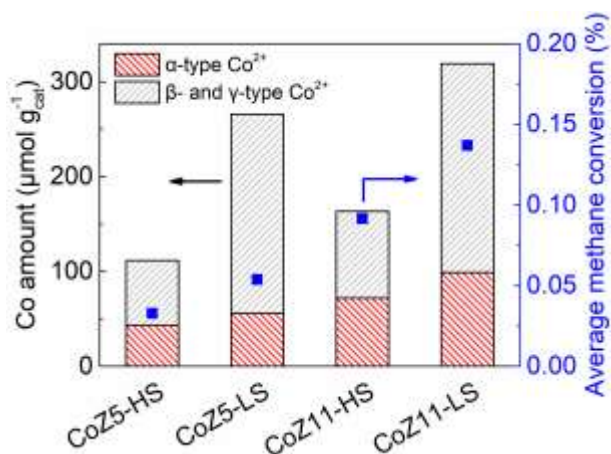


**Fig. 8.** Relation between Co amount ( $\alpha$ -type  $\text{Co}^{2+}$ , and  $\beta$ - and  $\gamma$ -type  $\text{Co}^{2+}$ ) and average methane conversion in initial 8 hours of the methylation of benzene with methane at 540 °C on various catalysts ( $F_{\text{He}}$ ,  $F_{\text{CH}_4}$  and  $F_{\text{C}_6\text{H}_6}$  = 84.6, 1230 and 53.1  $\mu\text{mol min}^{-1}$ , respectively, and  $\text{WHSV}_{\text{C}_6\text{H}_6}$  = 0.83  $\text{h}^{-1}$ ).

#### 4. Conclusion

This study demonstrated the non-oxidative methylation of benzene with methane catalyzed by cobalt-exchanged ZSM-11 zeolite catalysts for the first time. Higher number of cobalt cations could be loaded in ZSM-11 zeolites than in ZSM-5 zeolites with the same Si/Al molar ratio, though they were synthesized with the same reactant composition (but different OSDAs) and procedure, and higher toluene formation rates and turnover frequencies were observed on cobalt-exchanged ZSM-11 catalysts. Furthermore, compared with high silica zeolite catalysts, low silica zeolite catalysts displayed superior methylation selectivity, and therefore had less coke depositions. According to the DR Vis-NIR spectra, divalent cobalt cations were primarily located at two kinds of ion exchange sites with different coordination states in both types of zeolites. The amount of the  $\alpha$ -type  $\text{Co}^{2+}$  with loose coordination to the framework oxygen atoms was found to have a positive correlation to the methane conversion ability, indicating its important role in the target catalytic reaction. The present results manifested that ZSM-11 zeolites could create more  $\alpha$ -type  $\text{Co}^{2+}$  than ZSM-5 zeolites with the same Si/Al molar ratio, making cobalt-exchanged ZSM-11 zeolites promising

for the methylation of benzene with methane under non-oxidative conditions. Further insights are required to discern the detailed relationship between the properties of the active cobalt species, such as coordination states and Lewis acidity, and the catalytic performance.

### **CRedit authorship contribution statement**

**Peidong Hu:** Methodology, Investigation, Formal analysis, Validation, Data curation, Visualization, Writing - original draft. **Koshiro Nakamura:** Methodology, Investigation, Formal analysis, Validation, Data curation. **Hitoshi Matsubara:** Methodology, Investigation, Formal analysis, Validation, Data curation. **Kenta Iyoki:** Resources, Supervision, Visualization, Writing - review & editing. **Yutaka Yanaba:** Investigation. **Kazu Okumura:** Investigation, Formal analysis. **Tatsuya Okubo:** Resources, Writing - review & editing. **Naonobu Katada:** Methodology, Resources, Conceptualization, Supervision, Project administration, Funding acquisition, Visualization, Writing - review & editing. **Toru Wakihara:** Methodology, Resources, Conceptualization, Supervision, Project administration, Funding acquisition, Visualization, Writing - review & editing.

### **Declaration of interests**

The authors declare that they have no known competing financial interests or personal relationships that could have appeared to influence the work reported in this paper.

### **Acknowledgement**

This work was supported by JST CREST Grant Number JPMJCR17P1, Japan. The financial support from China Scholarship Council (CSC, File No. 201706230216) was also greatly appreciated.

## Reference

- [1] E. Tirronen, T. Salmi, *Chem. Eng. J.* 91 (2003) 103-114.
- [2] J. Van der Mynsbrugge, M. Visur, U. Olsbye, P. Beato, M. Bjørgen, V. Van Speybroeck, S. Svelle, *J. Catal.* 292 (2012) 201-212.
- [3] M. Adebajo, M.A. Long, R.L. Frost, *Catal. Commun.* 5 (2004) 125-130.
- [4] P. Tang, Q. Zhu, Z. Wu, D. Ma, *Energ. Environ. Sci.* 7 (2014) 2580-2591.
- [5] X. Guo, G. Fang, G. Li, H. Ma, H. Fan, L. Yu, C. Ma, X. Wu, D. Deng, M. Wei, D. Tan, R. Si, S. Zhang, J. Li, L. Sun, Z. Tang, X. Pan, X. Bao, *Science* 344 (2014) 616-619.
- [6] S. Mukhopadhyay, A.T. Bell, *Angew. Chem. Int. Ed.* 42 (2003) 1019-1021.
- [7] X. Wang, J. Xu, G. Qi, B. Li, C. Wang, F. Deng, *J. Phys. Chem. C* 117 (2013) 4018-4023.
- [8] M. Adebajo, M.A. Long, R.F. Howe, *Res. Chem. Intermed.* 26 (2000) 185-191.
- [9] M.O. Adebajo, R.L. Frost, *Energ. Fuel.* 19 (2005) 783-790.
- [10] M.O. Adebajo, *Green Chem.* 9 (2007) 526-539.
- [11] Q. Zhang, D. He, Q. Zhu, *J. Energy Chem.* 12 (2003) 81-89.
- [12] M.B. Park, E.D. Park, W.S. Ahn, *Front. Chem.* 7 (2019) 514.
- [13] H. Sheng, E.P. Schreiner, W. Zheng, R.F. Lobo, *ChemPhysChem* 19 (2018) 504-511.
- [14] Y. Xiao, A. Varma, *ACS Catal.* 8 (2018) 2735-2740.
- [15] D.B. Lukyanov, T. Vazhnova, *J. Mol. Catal. A: Chem.* 305 (2009) 95-99.
- [16] A.A. Gabrienko, S.S. Arzumanov, I.B. Moroz, I.P. Prosvirin, A.V. Toktarev, W. Wang, A.G. Stepanov, *J. Phys. Chem. C* 118 (2014) 8034-8043.
- [17] A.A. Gabrienko, S.S. Arzumanov, I.B. Moroz, A.V. Toktarev, W. Wang, A.G. Stepanov, *J. Phys. Chem. C* 117 (2013) 7690-7702.
- [18] K. Nakamura, A. Okuda, K. Ohta, H. Matsubara, K. Okumura, K. Yamamoto, R. Itagaki, S. Suganuma, E. Tsuji, N. Katada, *ChemCatChem* 10 (2018) 3806-3812.
- [19] H. Matsubara, E. Tsuji, Y. Moriwaki, K. Okumura, K. Yamamoto, K. Nakamura,

- S. Suganuma, N. Katada, *Catal. Lett.* 149 (2019) 2627-2635.
- [20] C. Peng, Z. Liu, Y. Yonezawa, Y. Yanaba, N. Katada, I. Murayama, S. Segoshi, T. Okubo, T. Wakihara, *Micropor. Mesopor. Mater.* 277 (2019) 197-202.
- [21] Z. Liu, K. Okabe, C. Anand, Y. Yonezawa, J. Zhu, H. Yamada, A. Endo, Y. Yanaba, T. Yoshikawa, K. Ohara, T. Okubo, T. Wakihara, *Proc. Natl. Acad. Sci. U.S.A.* 113 (2016) 14267-14271.
- [22] P.A. Jacobs, H.K. Beyer, J. Valyon, *Zeolites* 1 (1981) 161-168.
- [23] H. Liu, S. Liu, S. Xie, C. Song, W. Xin, L. Xu, *Catal. Lett.* 145 (2015) 1972-1983.
- [24] J.L. Sotelo, M.A. Uguina, J.L. Valverde, D.P. Serrano, *Ind. Eng. Chem. Res.* 35 (1996) 1300-1306.
- [25] K. Nakamura, K. Okumura, E. Tsuji, S. Suganuma, N. Katada, *ChemCatChem* 12 (2020) 2333-2340.
- [26] Y. Shen, T.T. Le, R. Li, J.D. Rimer, *ChemPhysChem* 19 (2018) 529-537.
- [27] P. Sazama, B. Wichterlova, J. Dedecek, Z. Tvaruzkova, Z. Musilova, L. Palumbo, S. Sklenak, O. Gonsiorova, *Micropor. Mesopor. Mater.* 143 (2011) 87-96.
- [28] J. Brus, L. Kobera, W. Schoefberger, M. Urbanova, P. Klein, P. Sazama, E. Tabor, S. Sklenak, A.V. Fishchuk, J. Dedecek, *Angew. Chem. Int. Ed.* 54 (2015) 541-545.
- [29] L. Shirazi, E. Jamshidi, M.R. Ghasemi, *Cryst. Res. Technol.* 43 (2008) 1300-1306.
- [30] Y. Guo, Y. Zhang, Z. Zhao, *Chin. J. Catal.* 39 (2018) 181-189.
- [31] L. Li, X. Cui, J. Li, J. Wang, *J. Braz. Chem. Soc.* 26 (2015) 290-296.
- [32] J. Dedecek, V. Balgová, V. Pashkova, P. Klein, B. Wichterlová, *Chem. Mater.* 24 (2012) 3231-3239.
- [33] L.V.C. Rees, in: A. Dyer, H. M.J., P.A. Williams (Eds.), *Progress in Ion Exchange: Advances and Applications*, The Royal Society of Chemistry, Cambridge, 1997, pp. 393-402.
- [34] J. Dědeček, D. Kaucký, B. Wichterlová, *Micropor. Mesopor. Mater.* 35-36 (2000) 483-494.
- [35] J.H. Shen, A.C. Zettlemoyer, K. Klier, *J. Phys. Chem.* 84 (1980) 1453-1459.
- [36] J. Dědeček, B. Wichterlová, *J. Phys. Chem. B* 103 (1999) 1462-1476.
- [37] J. Dědeček, L. Čapek, D. Kaucky, Z. Sobalik, B. Wichterlova, *J. Catal.* 211 (2002)

198-207.

[38] S. Wang, L. Zhang, S. Li, Z. Qin, D. Shi, S. He, K. Yuan, P. Wang, T.-S. Zhao, S. Fan, M. Dong, J. Li, W. Fan, J. Wang, *J. Catal.* 377 (2019) 81-97.

[39] P. Xie, Y. Luo, Z. Ma, L. Wang, C. Huang, Y. Yue, W. Hua, Z. Gao, *Appl. Catal. B: Environ.* 170-171 (2015) 34-42.

[40] A. Janda, A.T. Bell, *J. Am. Chem. Soc.* 135 (2013) 19193-19207.

[41] X. Su, W. Zan, X. Bai, G. Wang, W. Wu, *Catal. Sci. Technol.* 7 (2017) 1943-1952.

[42] M. Cai, A. Palčić, V. Subramanian, S. Moldovan, O. Ersen, V. Valtchev, V.V. Ordonsky, A.Y. Khodakov, *J. Catal.* 338 (2016) 227-238.

[43] E. Broclawik, K. Gora-Marek, M. Radon, T. Bucko, A. Stepniewski, *J. Mol. Model.* 23 (2017) 160.

[44] G. Ye, Y. Sun, Z. Guo, K. Zhu, H. Liu, X. Zhou, M.-O. Coppens, *J. Catal.* 360 (2018) 152-159.

[45] Y. Lou, J. Ma, W. Hu, Q. Dai, L. Wang, W. Zhan, Y. Guo, X.-M. Cao, Y. Guo, P. Hu, G. Lu, *ACS Catal.* 6 (2016) 8127-8139.